INSTITUTE OF PHYSICS PUBLISHING SMART MATERIALS AND STRUCTURES
Smart Mater. Struct. **10** (2001) 305–313 www.iop.org/Journals/sm PII: S0964-1726(01)20963-X

Design of actuator profiles for minimum power consumption

A Mukherjee and S P Joshi

Department of Civil Engineering, Indian Institute of Technology, Bombay, Powai - 400 076, Mumbai, India

Received 16 June 2000, in final form 15 November 2000

Abstract
The power consumption of piezoelectric actuators for active control is an important parameter for the efficient performance of a smart structural system. In this paper we address the issue of minimizing the maximum power consumption by the efficient layout of the actuators to achieve a specified maximum displacement. The finite element method is used for the structural response of piezoelectric composite plates under mechanical and electrical loading. A novel iterative design procedure based on the work done by the actuators on the host structure is presented. The voltage required to achieve the maximum displacement is calculated for changing actuator profiles and the peak power consumed by the actuators is determined. Although the method is general and can be applied to dynamic conditions, the scope of the present paper is restricted to static analysis only. Several numerical examples with simple and complex boundary conditions are presented.

(Some figures in this article are in colour only in the electronic version; see `www.iop.org`)

1. Introduction

Piezoelectric materials are extensively used as sensors and actuators because they couple electrical energy with mechanical energy. In the design of aerospace, automotive and civil structures, these materials are being introduced to create high-performance structures that are light, energy efficient and autonomous. Several studies have been carried out on active vibration control, noise suppression and instability control. The adjustment of shape of reflector antennae and deformable mirrors are some important applications of shape control under static conditions. An important parameter for the efficient performance of these structures is the power consumption while meeting the design requirements. In many practical cases only a limited power supply may be available. It would be ideal if we were able to achieve the desired displacements in the structure using as little power as possible. Thus, we would be interested in minimizing the maximum power required for the control of the structure. In such situations it is important to have an actuator configuration such that the power consumption is minimal. In this paper we consider the problem of finding actuator configurations that consume the least power for piezo-laminated plate structures with various boundary conditions. Although the present method is general and it can be applied under dynamic conditions, in this paper we present the results for static cases.

Several researchers have studied optimal sensor and actuator placement problems. Padula and Kincaid [1] surveyed sensor/actuator placement problems and their solution methods in detail. The methods surveyed vary from intuitive placement recipes to numerical optimization problems. Ryou *et al* [2] presented a procedure for electrode pattern designs of piezoelectric sensors and actuators using a genetic algorithm. They discussed the effect of electrode shape on the performance of the system. The actuator design is based on the criterion of minimizing the system energy in the control modes. The sensor is designed to minimize the observation spillover. Zuang and Baras [3] addressed the problem of obtaining optimal actuator layout for the active vibration control of beams. The energy functional is minimized over admissible shape functions space subject to certain geometric constraints. Gaudenzi and Barboni [4] presented analytical solutions for the static adjustment of beam deflections using induced strain actuation. They applied two deformation constraints on beams so that the two unknowns (the location and the size of the actuator) can be determined uniquely.

Some researchers have studied the power requirements of piezoelectric materials. Brennan and McGowan [5] presented a method for predicting the power consumption of piezoelectric actuators. The authors stated that the maximum power required is independent of the dynamics between the

 © 2001 IOP Publishing Ltd Printed in the UK

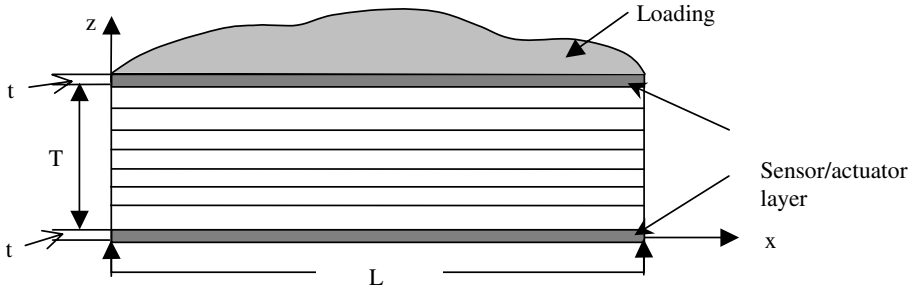

Figure 1. Cross section of a composite plate with bonded piezoelectric layers.

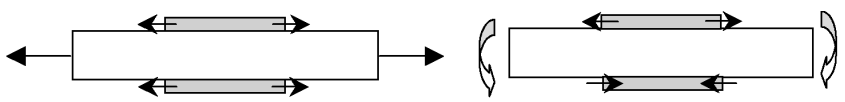

Figure 2. In- and out-of-phase actuation modes: (*a*) in-phase actuation mode (extensional) and (*b*) out-of-phase actuation mode (bending).

actuator and the host structure when the structure is perfectly controlled. Wise and Hooker [6] carried out experimental analysis to characterize commercially available piezoelectric actuators. They investigated the actuators based on their power consumption, displacement properties and electromechanical coupling coefficients. The authors have highlighted the importance of low power consumption in practical situations.

The aim of this paper is to obtain an actuator layout that gives minimum power consumption in order to achieve a specified displacement of a plate. Conversely, the problem can be stated as a search for an actuator configuration that would lead to maximum actuation for a specified applied voltage. The plate behavior is investigated under static conditions. A novel iterative procedure for obtaining actuator patterns is presented. The procedure is based on the work done by the actuators in achieving the specified displacement of the plate. We briefly present the finite element formulation for the static response of the piezo-laminated composite plates.

2. Mathematical model

A laminated plate with integrated piezoelectric layers is shown in figure 1. The sensor and actuator layers can be surface bonded or embedded. The constitutive relations for piezo-laminated composite plate are

$$\boldsymbol{\sigma}_{ij} = \overline{\boldsymbol{D}}(\varepsilon_{ij} - \boldsymbol{\alpha}\Delta T) - (\boldsymbol{e}^T \boldsymbol{E}_j) \tag{1}$$

$$\boldsymbol{D}_j = \boldsymbol{e}\varepsilon_{ij} + \overline{\varepsilon}\boldsymbol{E}_j \tag{2}$$

where $\boldsymbol{\varepsilon}$ is the mechanical strain vector, ε_{ij} is the mechanical strain of ith surface in jth direction; $\boldsymbol{\sigma}$ is the stress vector induced by mechanical, electrical and thermal effects; $\boldsymbol{D}$ is the electric displacement vector; $\boldsymbol{E}$ is the electric field vector, E_j is the electric field strength in jth direction; $\overline{\boldsymbol{D}}$ is the matrix of elastic constants; $\boldsymbol{e}$ is the matrix of piezoelectric constants; $\overline{\varepsilon}$ is the matrix of dielectric constants; $\Delta\boldsymbol{T}$ is the temperature change from reference state; and $\boldsymbol{\alpha}$ is the transformed thermal expansion coefficient matrix. Equations (1) and (2) are linear relations for a piezoelectric continuum and they represent the converse and direct piezoelectric effects respectively. These equations are written in extended form as follows:

$$\begin{Bmatrix} \sigma_1 \\ \sigma_2 \\ \tau_{23} \\ \tau_{13} \\ \tau_{12} \end{Bmatrix}_k = \begin{bmatrix} Q_{11} & Q_{12} & 0 & 0 & Q_{16} \\ Q_{12} & Q_{22} & 0 & 0 & Q_{26} \\ 0 & 0 & Q_{33} & Q_{34} & 0 \\ 0 & 0 & Q_{34} & Q_{44} & 0 \\ Q_{16} & Q_{26} & 0 & 0 & Q_{66} \end{bmatrix}_k \times \begin{Bmatrix} \varepsilon_1 - \alpha_1\Delta T \\ \varepsilon_1 - \alpha_2\Delta T \\ \gamma_{23} \\ \gamma_{13} \\ \varepsilon_{12} - \alpha_{12}\Delta T \end{Bmatrix} - \begin{bmatrix} 0 & 0 & e_{31} \\ 0 & 0 & e_{32} \\ 0 & e_{24} & 0 \\ e_{15} & 0 & 0 \\ 0 & 0 & 0 \end{bmatrix} \begin{Bmatrix} 0 \\ 0 \\ E_3 \end{Bmatrix} \tag{3}$$

$$\begin{Bmatrix} D_1 \\ D_2 \\ D_3 \end{Bmatrix} = \begin{bmatrix} 0 & 0 & 0 & e_{15} & 0 \\ 0 & 0 & e_{24} & 0 & 0 \\ e_{31} & e_{32} & 0 & 0 & 0 \end{bmatrix} \begin{Bmatrix} \varepsilon_1 \\ \varepsilon_2 \\ \gamma_{23} \\ \gamma_{13} \\ \gamma_{12} \end{Bmatrix} + \begin{bmatrix} \bar{\varepsilon}_{11} & 0 & 0 \\ 0 & \bar{\varepsilon}_{22} & 0 \\ 0 & 0 & \bar{\varepsilon}_{33} \end{bmatrix} \begin{Bmatrix} 0 \\ 0 \\ E_3 \end{Bmatrix} \tag{4}$$

3. Finite element model

In the present work an eight-node C_0 - continuous plate element is employed. The displacement field based on first-order shear-deformation theory is given as

$$u(x, y, z, t) = u_0 - z\theta_y(x, y, t)$$

$$v(x, y, z, t) = v_0 + z\theta_x(x, y, t)$$

$$w(x, y, z, t) = w_0(x, y, t). \tag{5}$$

The terms u_0, v_0 and w_0 are the mid-plane displacements and θ_x and θ_y are the rotations of transverse normal about the x- and y-axes. Using isoparametric relationships, the coordinates and displacements inside the element are defined as

$$x_i = \sum_{i=1}^{n} N_i x_i \qquad y_i = \sum_{i=1}^{n} N_i y_i \qquad \delta = \sum_{i=1}^{n} N_i \delta_i \tag{6}$$

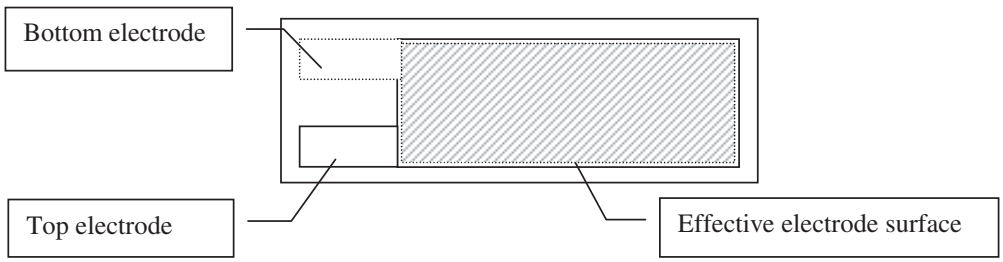

Figure 3. The surface area of an effective electrode.

where the N_i's are the element shape functions and n is the number of nodes per element.

The laminated piezoelectric plate equations are obtained by integration of equation (3) through the thickness we get

$$\begin{Bmatrix} \boldsymbol{N} \\ \boldsymbol{M} \end{Bmatrix} = \begin{bmatrix} \boldsymbol{A} & \boldsymbol{B} \\ \boldsymbol{B} & \boldsymbol{D} \end{bmatrix} \begin{Bmatrix} \varepsilon \\ \kappa \end{Bmatrix} - \begin{Bmatrix} \boldsymbol{N}^T \\ \boldsymbol{M}^T \end{Bmatrix} - \begin{Bmatrix} \boldsymbol{N}^P \\ \boldsymbol{M}^P \end{Bmatrix}$$

$$\begin{Bmatrix} \boldsymbol{Q}_x \\ \boldsymbol{Q}_y \end{Bmatrix} = \begin{bmatrix} \boldsymbol{S}_{44} & \boldsymbol{S}_{45} \\ \boldsymbol{S}_{54} & \boldsymbol{S}_{55} \end{bmatrix} \begin{Bmatrix} \gamma_{xz} \\ \gamma_{yz} \end{Bmatrix}. \tag{7}$$

The matrices $\boldsymbol{A}$, $\boldsymbol{B}$, $\boldsymbol{D}$ and $\boldsymbol{S}$ are the usual extensional, extension–bending coupling, bending and transverse shear stiffnesses of a plate. $\boldsymbol{N}^T$, $\boldsymbol{M}^T$, $\boldsymbol{N}^P$ and $\boldsymbol{M}^P$ are the generalized stress resultants due to thermal and piezoelectric effects.

3.1. Actuator mechanics

If the voltage is applied only in the thickness direction, the electric field intensity $(E_3)_k$ in the above equation is expressed as

$$(E_3)_k = \frac{V_k}{h_k} \tag{8}$$

where V_k is the applied voltage across kth layer and h_k is the thickness of the kth layer. The equivalent actuator force and moment resultants are

$$\begin{Bmatrix} N_x^P & M_x^P \\ N_y^P & M_y^P \\ N_{xy}^P & M_{xy}^P \end{Bmatrix} = \sum_{k=1}^{Nlay} \int_{z(k-1)}^{z(k)} \begin{Bmatrix} e_{31} \\ e_{32} \\ 0 \end{Bmatrix} \{l, z\}(E_3)_k \, \mathrm{d}z. \tag{9}$$

Care needs to be taken while performing the necessary integration to obtain the correct stiffness and actuator forcing terms. Both actuator and substrate plies contribute to stiffnesses, whereas only actuator plies contribute to forcing vectors. The actuator forcing terms are dependent on the mode of actuation, which may be extensional or bending (see figure 2).

Writing the potential energy equation,

$$\pi = \frac{1}{2}\Bigg(\iint_A \{ \varepsilon^{0\mathrm{t}} \quad \kappa^t \} \begin{bmatrix} \boldsymbol{A} & \boldsymbol{B} \\ \boldsymbol{B} & \boldsymbol{D} \end{bmatrix} \begin{Bmatrix} \varepsilon^0 \\ \boldsymbol{\kappa} \end{Bmatrix} \mathrm{d}\boldsymbol{A} - \Bigg(\iint_A [\, \boldsymbol{N}^T \quad \boldsymbol{M}^T \,] \begin{Bmatrix} \varepsilon^0 \\ \boldsymbol{\kappa} \end{Bmatrix} \mathrm{d}\boldsymbol{A} - \iint_A [\, \boldsymbol{N}^p \quad \boldsymbol{M}^p \,] \begin{Bmatrix} \varepsilon^0 \\ \boldsymbol{\kappa} \end{Bmatrix} \mathrm{d}\boldsymbol{A} \Bigg) \Bigg). \tag{10}$$

the strain-displacement relation is expressed in the form

$$\begin{Bmatrix} \varepsilon^0 \\ \kappa \end{Bmatrix} = \boldsymbol{B}\boldsymbol{\delta}_e \tag{11}$$

where $\boldsymbol{B}$ is the strain–displacement matrix. Equation (10) is written in concise form as

$$\pi = \frac{1}{2} \int_v (\boldsymbol{\delta}_e^T \boldsymbol{K} \boldsymbol{\delta}_e - \overline{\boldsymbol{F}} \boldsymbol{\delta}_e) \, \mathrm{d}V \tag{12}$$

where,

$$\boldsymbol{K} = \iint_A \boldsymbol{B}^T \overline{\boldsymbol{D}} \boldsymbol{B} \, \mathrm{d}A \qquad \overline{\boldsymbol{F}} = \boldsymbol{F} + \boldsymbol{F}^T + \boldsymbol{F}^P$$

$$\boldsymbol{F}^P = \iint_A \boldsymbol{B}^T \begin{Bmatrix} \boldsymbol{N}^P \\ \boldsymbol{M}^P \end{Bmatrix} \mathrm{d}A \qquad \boldsymbol{F}^T = \iint_A \boldsymbol{B}^T \begin{Bmatrix} \boldsymbol{N}^T \\ \boldsymbol{M}^T \end{Bmatrix} \mathrm{d}A$$

$$\boldsymbol{F} = \iint_A \boldsymbol{N}^T p \, \mathrm{d}A. \tag{13}$$

Minimizing the potential energy expression with respect to δ_e,

$$\boldsymbol{K}\boldsymbol{\delta}_\mathrm{e} = \overline{\boldsymbol{F}} \tag{14}$$

where $\boldsymbol{K}$ is the global stiffness matrix, $\boldsymbol{\delta}_\mathrm{e}$ is the vector of unknown nodal displacements and $\overline{\boldsymbol{F}}$ is the global force vector comprising of body forces, surface forces, thermal forces and actuation forces. In the present work the inertial effects are neglected and the forces are time-independent.

3.2. Sensor mechanics

As the charge is collected only in the thickness direction, only the dielectric displacement in direction 3 is of interest. Moreover, it can be assumed that for a piezo layer acting as a sensor, the electric field in direction 3 is zero. Thus equation (2) can be modified as follows:

$$D_3^k = \boldsymbol{e}\boldsymbol{\varepsilon} \tag{15}$$

where

$$\boldsymbol{\varepsilon} = (\, \varepsilon_x \quad \varepsilon_y \quad 0 \quad \gamma_{yz} \quad \gamma_{xz} \quad \gamma_{xy} \,)^T \tag{16}$$

According to the Gauss law, the closed circuit charge measured through the electrodes of a sensor patch in kth layer is

$$q = \frac{1}{2}\Bigg[\int_R D_3^k \, \mathrm{d}A \Bigg]_{z=z_k} + \Bigg[\int_R D_3^k \, \mathrm{d}A \Bigg]_{z=z_{k-1}} \tag{17}$$

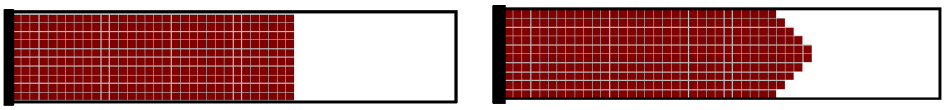

(*a*) (*b*)

Figure 4. Actuator configurations for minimum power (example 1): (*a*) e_{32} neglected and (*b*) e_{32} considered.

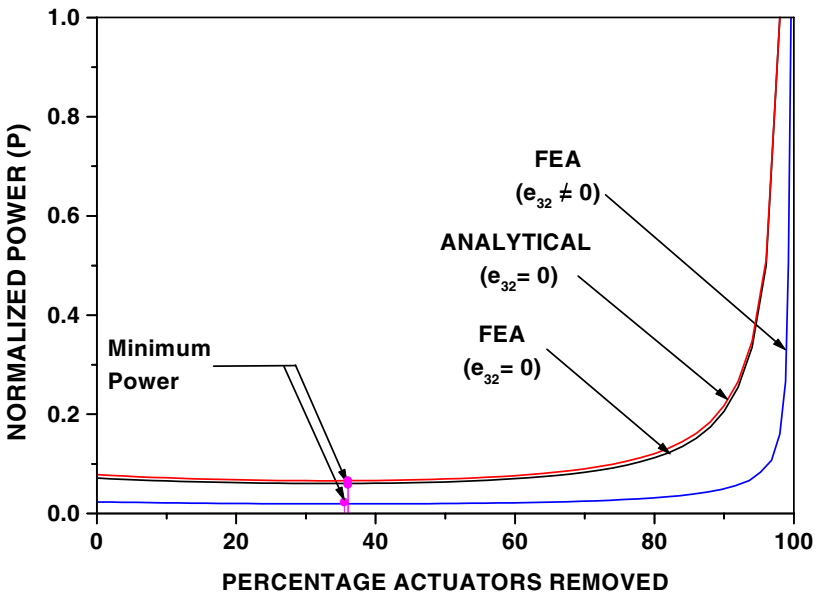

Figure 5. Variation of power with percentage actuator removal (example 1).

where R is the effective surface electrode of the patch. The effective area is the overlapping area of the electrode surfaces on both sides of the lamina (see figure 3). In the present analysis, it is assumed that the entire piezoelectric patch serves as an effective surface electrode. Using equation (15) in equation (17), we get

$$q = \int_R (\boldsymbol{eB\delta}_e)\,\mathrm{d}A \tag{18}$$

where $\boldsymbol{e}$ is a matrix of piezoelectric coefficients. The sensor voltage is computed as follows:

$$V_s = \frac{q}{C} \tag{19}$$

where $C = \bar{\varepsilon}A/t$ is the capacitance, $\bar{\varepsilon}$ is the permittivity, A is the active area of overlap of electrodes and t is the thickness of the piezoelectric patch.

4. Actuator shape design

In this work we present an iterative algorithm to obtain actuator profiles for specified boundary conditions. A sensitivity index based on the work done by the external loads and actuators is computed for each element. The actuators that are least sensitive are removed and the power requirement for the desired structural configuration is computed.

The system of equilibrium equations is

$$\boldsymbol{Ku} = \boldsymbol{P}. \tag{20}$$

If we neglect the change in stiffness due to removal of the ith actuator, equation (20) is modified as

$$\boldsymbol{Ku}^* = \boldsymbol{P}^* \tag{21}$$

where $\boldsymbol{K}$ is the global stiffness matrix, $\boldsymbol{u}$ is the original global displacement vector, $\boldsymbol{u}^*$ is the modified global displacement vector, $\boldsymbol{P}$ is the original global load vector, $\boldsymbol{P}^*$ is the modified global load vector. The change in displacement is

$$\boldsymbol{\Delta u} = (\boldsymbol{u}^* - \boldsymbol{u}) = \boldsymbol{K}^{-1}(\boldsymbol{P}^* - \boldsymbol{P}) \tag{22}$$

$$\boldsymbol{\Delta P} = (\boldsymbol{P} - \boldsymbol{P}^*). \tag{23}$$

The change in the work done is

$$\Delta W = (W^* - W) \tag{24}$$

$$\therefore \Delta W = [(\boldsymbol{P} - \boldsymbol{\delta P})^T(\boldsymbol{u} + \boldsymbol{\Delta u}) - (\boldsymbol{P}^T\boldsymbol{u})]. \tag{25}$$

Neglecting higher terms, the change in work done for the ith element is

$$\beta_i = |\Delta W| = [\boldsymbol{P}^T\boldsymbol{\Delta u} - \boldsymbol{\Delta P}^T\boldsymbol{u}]. \tag{26}$$

The sensitivity index is obtained as

$$\alpha_i = \left(1 - \frac{\beta_i}{\beta_{i,max}}\right) \tag{27}$$

where $\beta_{\mathrm{i},max}$ is the maximum value of β at the ith iteration.

The actuators with the lowest sensitivities are removed. In each iteration the peak power (P) consumed by the actuators to achieve a specified deflection is calculated. Due to the removal

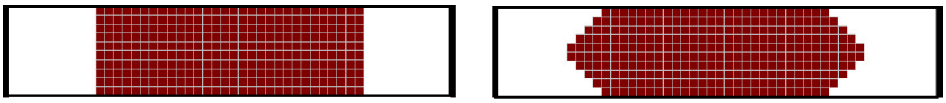

(*a*) (*b*)

Figure 6. Actuator configurations for minimum power (example 2): (*a*) e_{32} neglected and (*b*) e_{32} considered.

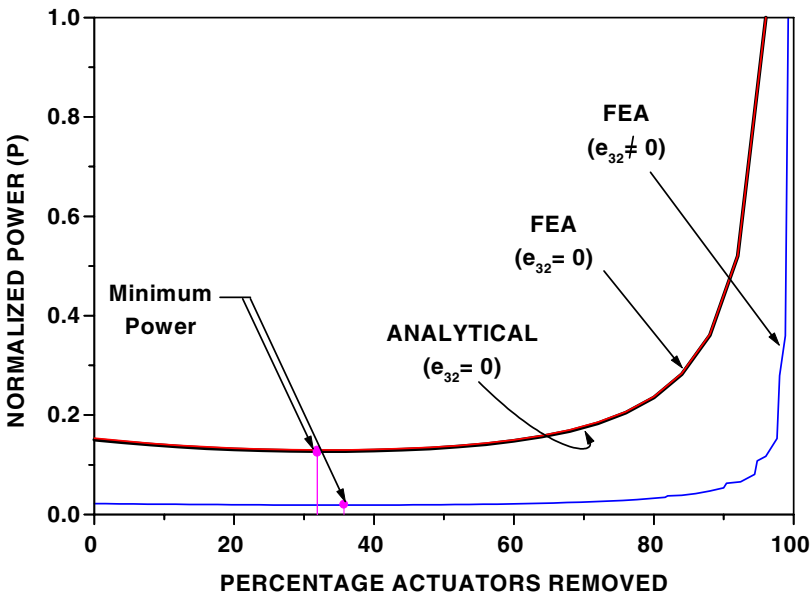

Figure 7. Variation of power with percentage actuator removal (example 2).

of certain actuator patches, the voltage required to achieve the same displacement changes and thus the power consumed by the actuators also changes. The actuator configuration that gives minimum power consumption is obtained. The actuator power consumption is given as

$$P = \pi f C V^2 \tag{28}$$

where f is the frequency (cycles per second), $C = \bar{\varepsilon} A/t$ is the capacitance of the actuator and V is the voltage.

Our objective is to find out an actuator configuration for a given structure such that the power consumed is minimal. In the present work we set the rate of actuator removal as 2% of the initial configuration that is fully populated. The actuators with sensitivity index (α) less than the critical value ($\alpha_c = 0.1$) are removed. The actuator removal rate is set such that a trade-off between the stability of the solution and the computational cost is achieved. The iterative process is summarized in the following steps.

(1) For the given finite element mesh and boundary conditions, solve the equilibrium equation (20).
(2) Calculate the sensitivity index (α) for each element using equation (27).
(3) Remove the actuators corresponding to lowest sensitivity indices using the set values of the actuator removal rate and the critical sensitivity index (α_c).
(4) Calculate the power consumed for a specified maximum displacement using equation (28).
(5) Repeat steps 2 to 4 until the objective function is satisfied.

To validate the above method we consider a few examples of the Euler–Bernoulli beams. For some of these structures the analytical expressions for power consumption can be derived. For a cantilever beam of length L with a specified tip deflection (δ), the power is expressed as

$$P = \pi f C \left(\frac{EI\delta}{e_{31} bhx(L - (x/2))} \right)^2 \tag{29}$$

where x is the length of actuator from fixed end. Similarly, considering a simply supported beam of length L with a specified central deflection (δ), the power consumed is given by

$$P = \pi f C \left(\frac{8EI\delta}{e_{31} bhx(x - 2L)} \right)^2 \tag{30}$$

where x is the length of the actuator placed symmetrically about the center of the beam. The values of power consumed for different values of x can be computed using the above equations and the length of the actuator corresponding to minimum power can be obtained. In the above equations (29) and (30) the piezoelectric effect e_{32} is neglected.

The present procedure is used to obtain actuator configurations for plates with different boundary conditions. In the next section we present the numerical results and make certain observations.

5. Numerical results and discussion

In this section we present some results for beams and plates with various boundary conditions under an electrical field.

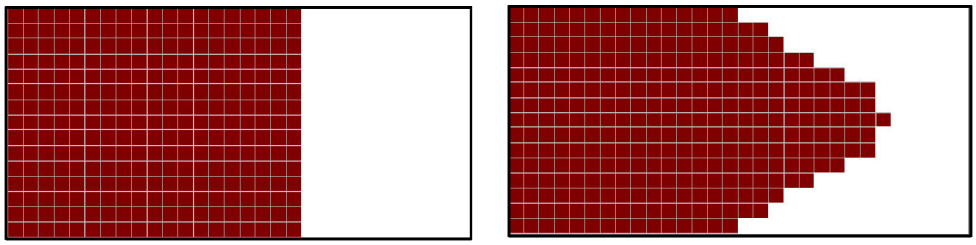

(*a*) (*b*)

Figure 8. Actuator configuration at minimum power (example 3): (*a*) e_{32} neglected and (*b*) e_{32} considered.

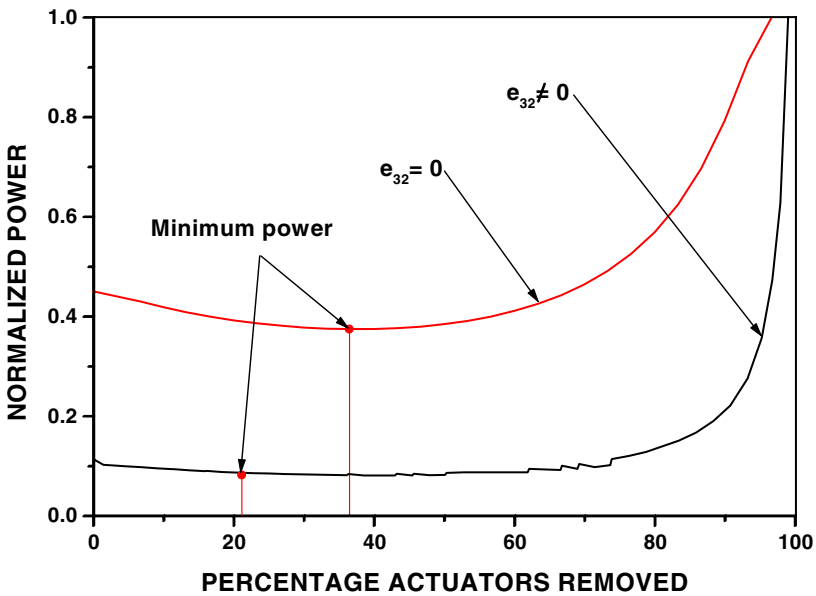

Figure 9. Variation of power with percentage actuator removal (example 3).

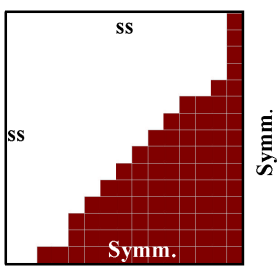

Figure 10. Actuator configuration at minimum power (example 4).

Table 1. Material properties.

Property	Piezoceramic	Aluminum
Young's modulii (GPa): E_1, E_2	63.0, 63.0	70.0
Poisson's ratio: ν_{12}	0.30	0.25
Shear modulii (GPa): G_{12}	24.20	28.00
Piezoelectric strain constants (pm V^{-1}): $d_{31} = d_{32}$, d_{33}	−256, 374	—
Thickness (mm)	0.25	0.50
Number of layers	2 (each at top and bottom)	2 (between the piezoelectric layers)

The first four examples are for simple boundary conditions, viz fixed–free and simple supports. In the fifth example we consider a complicated boundary condition, viz a plate fixed at one end and with an overhang at the other end. The material properties of the plate and the piezoelectric material are the same for all cases and are given in table 1. An initial electrical voltage of 1 V is applied and the voltage required to obtain the specified displacement is computed in each iteration.

5.1. Example 1: cantilever beam

A cantilever beam (0.1 m × 0.02 m) is modeled using 50 × 10 finite element mesh. The objective is to find the actuator configuration that gives the minimum power consumption and the corresponding voltage required to obtain the specified tip deflection (at the center of the tip) of 0.4×10^{-6} m. Figure 4(*a*) shows the actuator configuration corresponding to the minimum power required when the piezoelectric effect e_{32} is neglected. This piezoelectric effect is neglected in order to compare the results with those available from analytical results (equation (29)). Figure 5 shows the predicted power requirement with the different actuator configurations. The analytical and the finite element solutions correlate well. The voltage corresponding to the minimum power is 20 V. The percentage of actuator patches removed is 38% of the initial configuration that was fully populated.

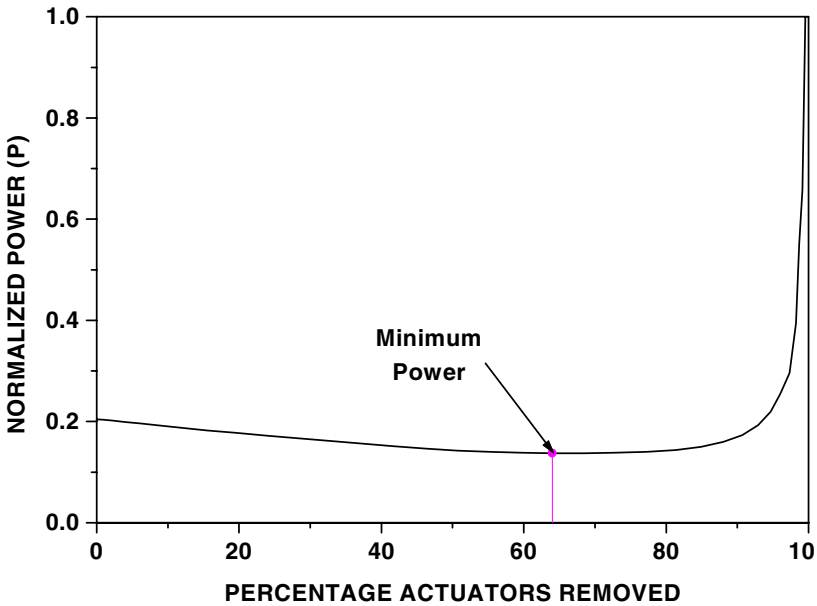

Figure 11. Variation of power with percentage actuator removal (example 4).

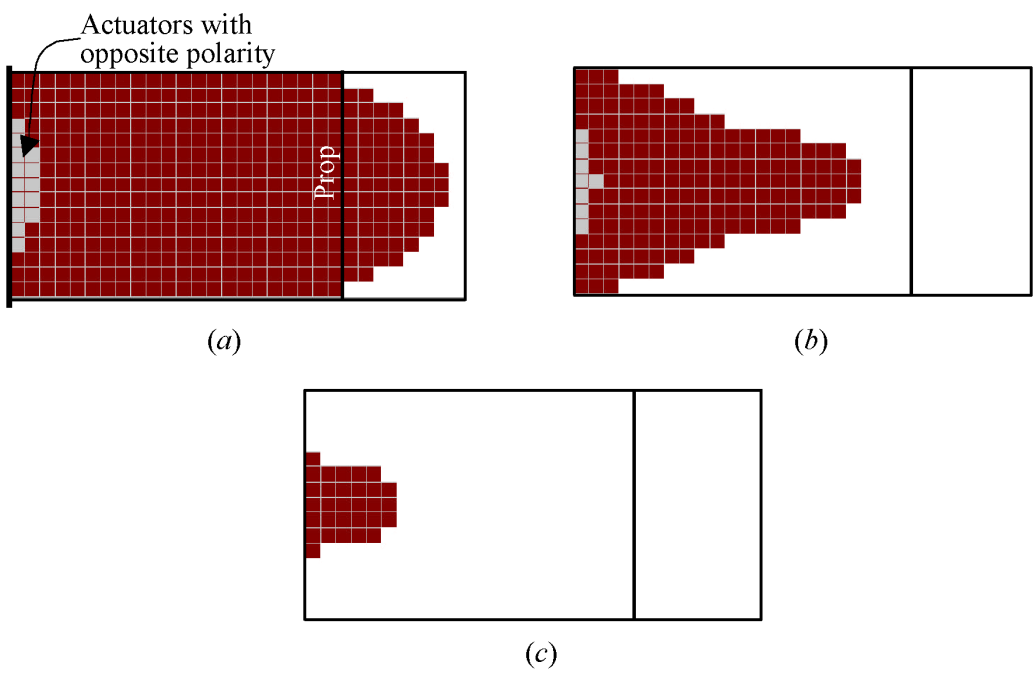

Figure 12. Actuator profiles at various percentage actuators removed (example 5): (*a*) at minimum power, (*b*) tip deflection close to zero, (*c*) 93% actuator patches removed.

The actuator configuration when e_{32} is considered is shown in figure 4(*b*). The actuator profile differs considerably when e_{32} is considered. The variation of the power requirement with varying actuator configurations is presented in figure 5. The voltage corresponding to this actuator configuration is 40 V and about 36% of the initial actuator patches are removed.

5.2. Example 2: simply supported beam

A beam, (0.1 m × 0.02 m), simply supported at two short edges, is modeled using a 50 × 10 finite element mesh. The objective is to find the actuator configuration that gives the minimum power consumption and the corresponding voltage for the specified central deflection of 0.4×10^{-6} m. Figure 6(*a*) shows the actuator configuration corresponding to the minimum power when the piezoelectric effect e_{32} is neglected. These results are compared with the analytical solution (equation (30)), and they match very well (figure 7). The voltage corresponding to the minimum power is 77 V. The percentage of actuator patches removed is 32% of the initial fully populated configuration.

The actuator configuration when e_{32} is considered is shown in figure 6(*b*). As in the previous example, the actuator configuration and the variation of the power requirement change considerably with the inclusion of e_{32} (figure 7). The voltage corresponding to this actuator configuration is 103 V and about 36% of the initial actuator patches are removed.

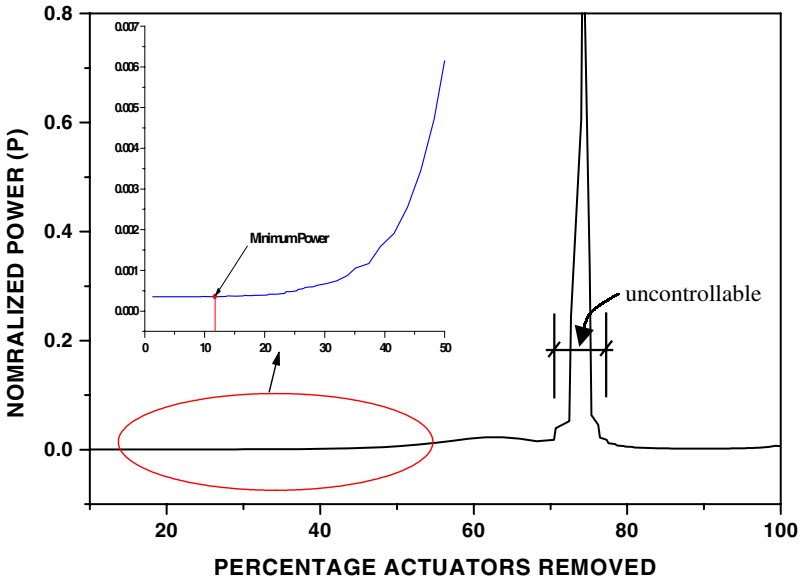

Figure 13. Variation of power with percentage actuator removal (example 5).

5.3. Example 3: cantilever plate

In the previous examples plates with large aspect ratios were considered so that the finite element results can be compared with the analytical solutions. In this example a cantilever plate of a smaller aspect ratio (0.2 m × 0.1 m) is considered. A tip deflection of 0.4×10^{-6} m is specified. The displacement is set at the center of the tip. The entire plate is discretized into a 30 × 15 finite element mesh. Figure 8(*a*) shows the actuator configuration for minimum power consumption when e_{32} is not considered. About 37% actuators of the initial fully populated actuator are removed. The voltage corresponding to this configuration is 4.9 V. Figure 9 shows the variation of the power with the percentage of actuators removed.

Figure 8(*b*) shows the actuator profile that gives the minimum power consumption when e_{32} is considered. About 21% of actuators are removed. The voltage corresponding to the minimum power is 6 V. The deviation in the power requirement with the inclusion of e_{32} increases as the plate becomes more square (figure 9). This emphasizes the importance of the inclusion of e_{32} in the design of the actuator profile for plates.

5.4. Example 4: simply supported plate

In this example a square plate, simply supported at all four edges, is considered. The objective is to find the actuator configuration and the voltage that give the minimum power consumption needed to obtain the specified deflection of 0.1×10^{-6} m at the center of the plate. A quarter model (0.1 m × 0.1 m) of the plate is discretized into a 15 × 15 finite element mesh. Figure 10 shows the actuator configuration for the minimum power requirement. The iteration was started with a fully populated initial configuration and 64% of actuator patches were removed for minimum power. Figure 11 shows the variation of power with changing actuator profiles. The voltage corresponding to minimum power is 48 V.

5.5. Example 5: propped cantilever with overhang

The cantilever plate in example 2 is propped at 0.14 m from the fixed end. The tip deflection at the center of the free end is specified as 0.4×10^{-6} m. Unlike the previous examples, in this example the plate has a point of contraflexure. Thus, the polarity of the voltage applied is opposite on either side of the point of contraflexure. In this example both e_{31} and e_{32} are considered. Figure 12(*a*) shows the actuator distribution corresponding to minimum power. About 12% of the initial actuator patches are removed. The voltage corresponding to the minimum power is 41 V. In figure 12(*b*) we see that as the actuator removal progresses the tip deflection reduces and nears a zero value. Such configurations can be termed as *dead* configurations because it would hardly be possible to control the plate with these configurations. At this point the voltage requirement to achieve the specified tip deflection is very high. Therefore, the power consumption increases rapidly. As the actuator removal continues further, the direction of the tip deflection changes (figure 12(*c*)). However, the direction of deflection can be controlled by swapping the polarity of the applied voltage. As a result, the power requirement decreases. However, the power requirement is still higher as compared to that in the initial stages of the process. This is primarily because a considerable number of actuator patches are removed and the voltage requirements are high. Therefore, even though the curve in figure 13 shows a drop, the configurations may not be feasible in practice.

6. Conclusions

In this paper we address the issue of minimizing the power consumed by actuators in the control of plate structures. An iterative procedure to derive the actuator configuration that requires the minimum power to achieve the desired displacements of the plate structures has been presented. It is seen from the numerical examples that, for given structure and actuator properties, we can find an actuator configuration that consumes minimum power. The results have been validated

with analytically obtained solutions. It is observed that e_{32} is an important parameter and it should not be neglected, especially for plates tending towards a square profile. In the case of structures with complex boundary conditions the power requirement varies rapidly with changing actuator configurations. It is very important to identify the actuator configurations that are effective in controlling the structure. Work on actuator profiles for dynamic control is in progress and shall soon be reported.

References

[1] Padula S L and Kincaid R K 1999 Optimization strategies for sensor and actuator placement *NASA Technical Memorandum* TM-1999-209126, pp 1–11

[2] Ryou J-K, Park K-Y and Kim S-J 1998 Electrode pattern design of piezoelectric sensors and actuators using genetic algorithms *AIAA J.* **36** 227–33

[3] Zuang Y and Baras J S 1993 Considerations on optimal design of distributed sensors and actuators of smart materials for active vibration control *Technical Research Report* TR 93-4 *Institute of Systems Research, University of Maryland*

[4] Gaudenzi P and Barboni R 1999 Static adjustment of beam deflections by means of induced strain actuators *Smart Mater. Struct.* **8** 278–83

[5] Brennan M C and McGowan A R 1997 Piezoelectric power requirements for active vibration control *Proc. SPIE 4th Ann. Symp. on Smart Structures and Materials (San Diego, CA)* pp 1–10

[6] Wise S A and Hooker M W 1997 Characterization of multilayer piezoelectric actuators for use in active isolation mounts *NASA Technical Memorandum* TM-4742